JOC The Journal of Organic Chemistry

pubs.acs.org/joc Article

How an Eight-Membered Ring Alters the Rhodamine Chromophore

Yevgen M. Poronik, Filip Ambicki, Sheng-Ming Tseng, Pi-Tai Chou,* Irena Deperasińska,* and Daniel T. Gryko*

Cite This: J. Org. Chem. 2020, 85, 5973−5980 Read Online

ACCESS | Metrics & More | Article Recommendations | Supporting Information

ABSTRACT: Readily available phenylene-1,3-diamines can be converted into unprecedented analogues of rhodamine and malachite green possessing a central eight-membered ring in three steps. The overall process couples a cyanine chromophore with a urea bridge giving rise to new dyes possessing distinct spectral characteristics: absorption of orange light combined with a weak emission of red light both in solution and in the crystalline state. Their photophysics is governed by the twist of lateral phenyl rings and intramolecular and intermolecular CT transitions.

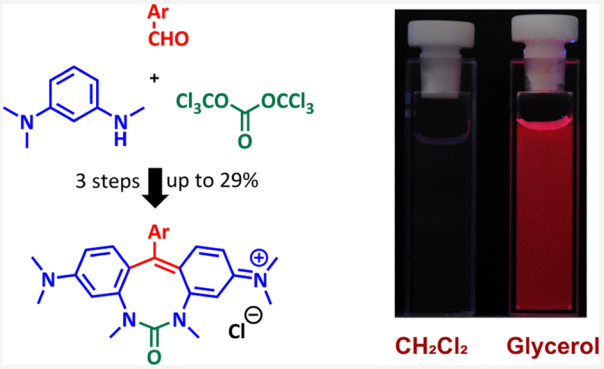

INTRODUCTION

The study of biological systems at the cellular and subcellular levels is greatly aided by small molecule fluorophores, of which members of the xanthene family, including fluorescein and rhodamine, have proved invaluable.[1] Recently, there has been an increased focus on harnessing the photophysical properties of these ubiquitous dyes through structural modifications. In particular, π-expansion[2−6] and replacement of the xanthene oxygen atom bridge with silicon,[7−9] phosphorus,[10] sulfur,[11] or carbon[12−14] in rhodamine,[15−18] fluorescein,[19,20] and rhodol[21] scaffolds have proved to be popular and effective.

The dyes from this extended family, despite their structural and functional diversity, share the quintessential characteristics: (a) planar aromatic structures; (b) excellent spectroscopic properties including strong absorption and fluorescence; (c) relatively small Stokes shifts; and (d) biocompatibility. At the same time, nonplanar chromophores, however, feature a number of peculiar properties, making it possible to overcome the limitations of conventional chromophores such as: (a) increased possibility for intramolecular charge transfer (ICT) and (b) their tendency to be more soluble, less aggregating, and be able to form amorphous thin films. The latter makes nonplanar chromophores good candidates for potential use in optoelectronic devices.[22,23]

The replacement of the oxygen bridge in xanthene chromophores with a two- or three-atom unit, which has not been reported to date, would enable us to create rigid but nonplanar chromophores. The concept of this project was to address the above general idea by constructing an analogue of rhodamine in which the bridging oxygen atom is formally replaced with a urea moiety to create an eight-membered ring. This can also be thought of as an analogue of malachite green (MG) in which the dialkylaminophenyl groups are tethered by urea. The inclusion of a ring of this size inside a chromophore is known to generate a distortion in planarity,[24] resulting in an overall twisted geometry because of the strained central fragment.[25−31] Through exploitation of this strategy, we demonstrate how this targeted introduction of structural diversity into well-known rhodamine chromophores can unlock solvent- and state-dependent photophysical properties.

RESULTS AND DISCUSSION

Scheme 1 details our proposed strategy to generate rhodamine analogues possessing a central urea-based eight-membered ring (8U-Rh) by taking advantage of the reactivity of electron-rich phenylene-1,3-diamines. In the first step, 1-dimethylamino-3-methylaminobenzene (**1**) smoothly reacts with 4-chlorobenzaldehyde in the presence of acetic acid as a catalyst to form a triarylmethane derivative **2a**. Optimization of the subsequent cyclization step proved challenging because of the formation of a strained eight-membered ring system. Employment of phosgene solution led to a cyclized product **3a** only in trace amounts as the high reactivity of phosgene results in low selectivity of this process. Indeed, mass spectrometry (MS) experiments suggest that the product of the addition to both secondary amino groups of a single triarylmethane forms even at −20 °C. The use of

Received: February 17, 2020
Published: April 7, 2020

https://dx.doi.org/10.1021/acs.joc.0c00414
J. Org. Chem. 2020, 85, 5973−5980

Scheme 1. Synthetic Route for Rhodamine Analogues 4a−e

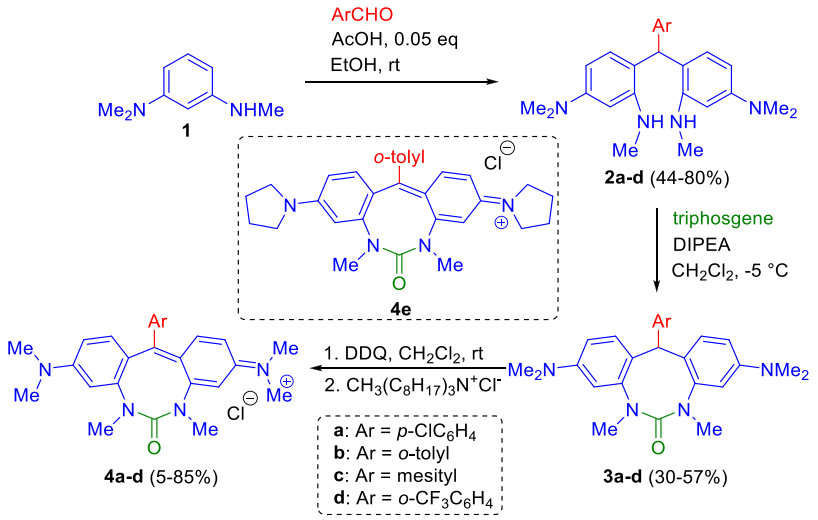

Table 1. Spectroscopic Properties of Urea-Bridged Rhodamines 4a−e in Solution

compd.	solvent	λ_{abs}/nm	$\varepsilon_{max} \times 10^{-3}/M^{-1}\ cm^{-1}$	λ_{em}/nm	$\Delta S^a/cm^{-1}$	Φ_{fl}
4a	DCM	595	71	635	1060	0.00068
	H_2O	584	41	[c]		0.00019
4b	DCM	589	71	635	1230	0.00044
	CH_3CN	580	50	[c]		0.00014
	H_2O	579	41	[c]		0.00010
	SOA[b]	586		637	1370	0.16
4c	DCM	587	68	637	1340	0.00148
	CH_3CN	579	48	[c]		0.00035
	H_2O	578	43	[c]		0.00017
	SOA[b]	583		638	1480	0.33
4d	DCM	600	58	656	1420	0.00058
	CH_3CN	590	41	[c]		0.00019
	H_2O	585	35	[c]		0.00009
4e	DCM	598	72	639	1070	0.00059
	CH_3CN	590	52	[c]		0.00050
	H_2O	590	39	[c]		0.00013
	SOA[b]	596		646	1300	0.17

[a]Stokes shift. [b]Compounds **4a** and **4d** decomposed during the SOA experiment. [c]Fluorescence maxima were not determined because of the extremely low emission response.

triphosgene, a less reactive analogue, enables a more selective initial reaction with a secondary amino group. According to MS data, experiments with different substrate/triphosgene ratios showed the formation of intermediates bearing triphosgene residues with different degrees of decomposition. The cyclization step is a much slower process and requires 3−18 days at room temperature in order to obtain the cyclic product **3a** bearing an eight-membered ring in 53% yield. The oxidation of compound **3a** with 2,3-dichloro-5,6-dicyanobenzoquinone (DDQ) leads to the formation of 8U-Rh **4a**.

To showcase our system's synthetic utility, this strategy was applied utilizing other aldehydes (Scheme 1). It was found that the efficacy of the cyclization reaction is dependent on both the steric hindrance (to a greater extent) and the electron-withdrawing properties of the aryl ring at the meso-position. Indeed, the reaction with 4-chlorobenzaldehyde was characterized by the shortest reaction time compared with that of 2-methylbenzaldehyde and mesitaldehyde; however, 2-trifluoromethylbenzaldehyde, which combined both these features, takes as long as 18 h to reach equilibrium. Further extension of the reaction time or variation of the temperature causes no improvement to the reaction yields. All in all, four additional 8U-Rhs **4b−e** were prepared in overall yields ranging from 1 to 21%.

In order to analyze the distorted nature of the synthesized dyes, the structures of chromophores **4b** and **4c** were determined by X-ray crystallography (Figures S1 and S2).

In the crystal lattice, molecules **4b** and **4c** adopt a curved chromophore structure with unsymmetric geometry. The lateral benzene rings are positioned at different dihedral angles related to the central chromophore plane ranging from 27 to 43° for **4b** and 29 to 32° for dye **4c**. Moreover, the dihedral angle between lateral benzene rings reaches 68° for **4b** and 60° for **4c,** respectively (Figure S3). This angle controls the mutual orientation of the chromophore molecules in the crystal lattice resulting in the minimal distances of 4.480 Å for **4b** and 3.591 Å for **4c,** respectively (Figure S4), between π-systems of adjacent molecules.

The absorption spectra of the urea-bridged xanthenes **4a−e** show intense maxima between 585 and 600 nm (Table 1, Figure 1). The influence of the electronic character of the central aryl

https://dx.doi.org/10.1021/acs.joc.0c00414
J. Org. Chem. 2020, 85, 5973−5980

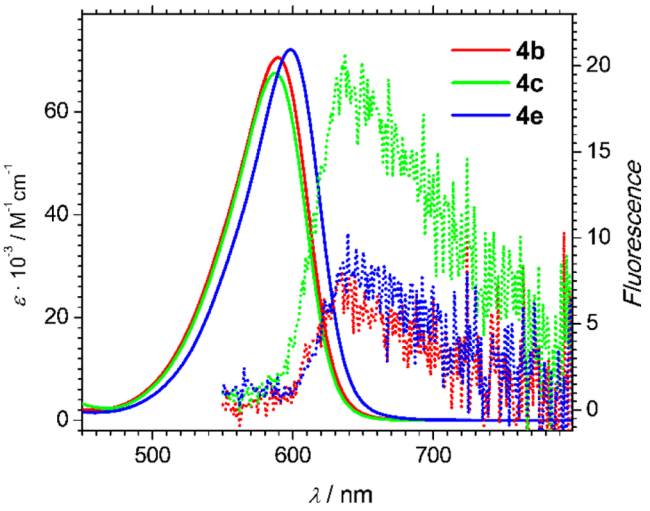

Figure 1. Absorption (solid) and fluorescence (dotted) spectra of compounds **4b**, **4c**, and **4e** in DCM.

substituent is rather weak. The 8U-Rhs **4a** and **4d** possessing moderately electron-withdrawing 4-chloro- and 2-trifluoromethylphenyl substituents display somewhat red-shifted absorption maxima at 595 and 600 nm respectively, while urea-bridged rhodamines with electron-donating aryl moieties (**4b,c**) demonstrate absorption in the range 587−589 nm. The solvent polarity moderately affects the absorption properties of 8U-Rhs. The nonpolar dichloromethane (DCM) dyes **4a**−**e** show more intense and more red-shifted absorption compared to acetonitrile and water solutions (Table 1).

The chromophore structure of 8U-Rhs resembles two known functional organic dyes, namely, rhodamine B (RB), possessing a rigid planar structure, and MG, which belongs to the triphenylmethane dye family. A comparison of spectral properties of 8U-Rhs **4a**−**e** with RB[32] shows that insertion of the "urea bridge" into the xanthene chromophore gives rise to a 35 nm bathochromic shift of the absorption maximum, while for MG,[33,34] the absorption is blue-shifted by 20 nm.

The fluorescence maxima of 8U-Rhs **4a**−**e** are typically around 635−640 nm, that is, they are ∼60 nm bathochromically shifted compared to RB. Regardless of the substitution pattern, 8U-Rhs **4a**−**e** are very weakly emissive, reminiscent of the picosecond fluorescence of MG.[35] Non-negligible Stokes shifts (Table 1, Figure 1) suggest certain geometrical differences between the molecules in their ground and excited states.

The hypothesis that the rotational motion of molecular fragments, in a similar manner to MG,[36−39] is the reason why 8U-Rhs show weak emission prompted us to study the dependence of fluorescence efficiency on the solution viscosity.[36] In methanol/glycerol mixtures, an increase in fluorescence efficiency was observed upon increasing the glycerol ratio (Figure 2, Table 2).

Likewise, stiffening of the environment by dissolution in highly viscous sucrose octaacetate (SOA)[40] limits the twisting of the 8U-Rhs' structure in the excited state, which results in a significant increase in the fluorescence efficiency. In SOA solutions, compounds **4b**, **4c**, and **4e** exhibit a 500−1000 fold increase in the fluorescence quantum yield with emission in a similar spectral region compared to traditional low viscous solvents (Figure 3, Table 1). This experiment unambiguously proves that rotations within the chromophore are responsible for the weak fluorescence of the "urea-bridged" rhodamines in

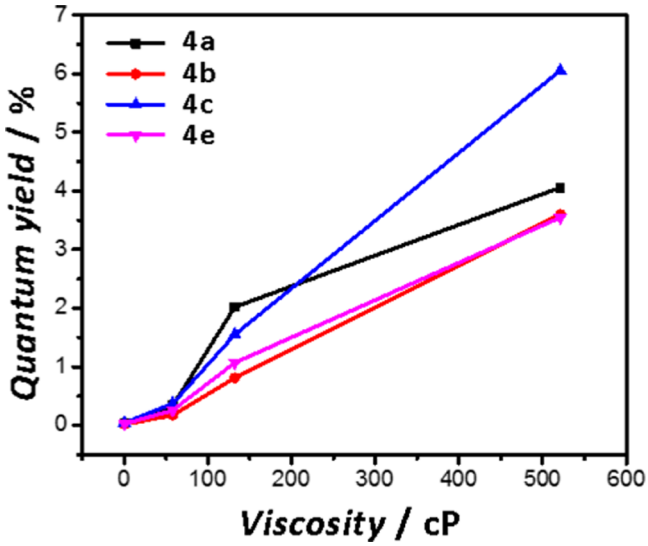

Figure 2. Dependence of the fluorescence quantum yield on the solution viscosity for 8U-Rhs in the methanol/glycerol mixture.

Table 2. Fluorescence Quantum Yields of 8U-Rh Solutions under Different Viscosity Environments

		Φ/%			
glycerol/MeOH volume ratio	η/cP	4a	4b	4c	4e
100:0	521.03	4.06	3.60	6.05	3.55
80:20	132.33	2.02	0.81	1.55	1.07
60:40	58.01	0.34	0.18	0.37	0.26
0:100	0.52	0.03	0.02	0.04	0.03

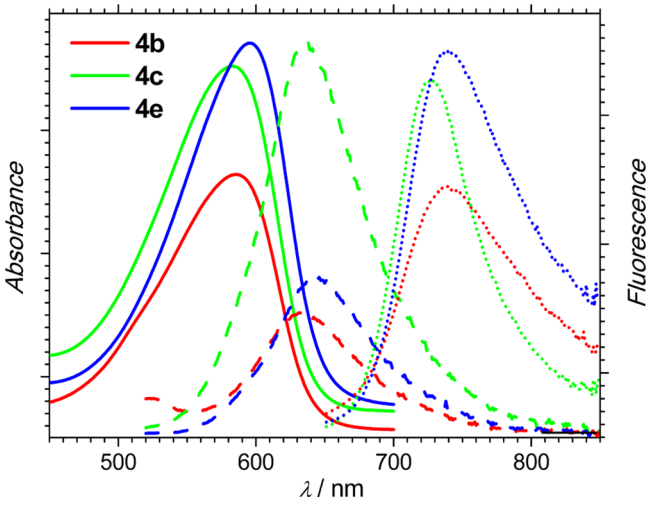

Figure 3. Absorption (solid) and fluorescence (dashed) spectra in SOA and fluorescence spectra in the polycrystalline state (dotted) for compounds **4b**, **4c**, and **4e**.

regular solvents. The fact that the electron-donating effect of the urea fragment is much weaker than that of nitrogen and comparable with the oxygen atom[41] reinforces a conclusion that the bent geometry rather than the presence of the nitrogen atom causes fluorescence quenching.

Fluorescence spectra were also recorded for 8U-Rhs in the polycrystalline state. Low fluorescence responses with peak wavelengths at 715 nm for **4a** (Φ = 0.22%), 740 nm for **4b** (Φ = 0.04%), 728 nm for **4c** (Φ = 0.15%), and 740 nm for **4e** (Φ =

https://dx.doi.org/10.1021/acs.joc.0c00414
J. Org. Chem. 2020, 85, 5973−5980

0.05%) were observed (Figure 3). The weak quantum yields lead us to suspect the self-quenching effect in the crystalline solid states, which may be associated with the size of the crystals. In this study, however, we found that there is no obvious difference in quantum yields between the polycrystalline and ground powder, as shown in Table S12. In comparison to the emission in solution, a >90 nm bathochromic shift is observed for the polycrystalline state, indicating that there is a strong influence of crystal packing on the emission properties, which causes the red shift and significant quenching of fluorescence.

To rationalize the photophysical processes, density functional theory (DFT) and time-dependent (TD) DFT/B3LYP/6-31G(d,p) and CAM-B3LYP/6-31G(d,p) calculations were performed for the geometry optimization of 8U-Rh cations in the ground and excited states. Also, to evaluate the solvent effect, the polarizable continuum model was adopted. The Supporting Information file includes additional calculation details and an overview of the calculation results.

Based on the data presented in Supporting Information (optimized structures, shapes of the corresponding molecular orbitals, energies, and oscillator strengths of electronic transitions for 8U-Rhs, RB, and MG), it can be seen that the calculations reproduce the similarity of the structures in addition to the mutual location of experimental absorption spectra of 8U-Rhs, RB, and MG (Tables S1 and 3), as well as the weak dependence of these spectra on solvent polarity (Table S2).

Table 3. $S_0 \rightarrow S_1$ and $S_1 \rightarrow S_0$ Transition Data for 4a−4d Cations and Ion Pairs in CH_3CN (TD B3LYP/6-31G(d,p))

	cations		ion pairs		
	$S_0 \rightarrow S_1$	$S_1 \rightarrow S_0$	$S_0 \rightarrow S_1$	$S_1 \rightarrow S_0$	
				(A)	(B)
4a	2.245 eV	0.954 eV	2.395 eV	0.3201 eV	1.466 eV
	552.18 nm	1300 nm	517.7 nm	3873 nm	845.6 nm
	f = 1.3751	f = 0.0003	f = 0.693	f = 0.000	f = 0.109
4b	2.276 eV	0.863 eV	2.2433 eV	0.894 eV	1.524 eV
	544.8 nm	1436 nm	552.7 nm	1386 nm	813.5 nm
	f = 1.300	f = 0.001	f = 1.1672	f = 0.001	f = 0.124
4c	2.285 eV	0.797 eV	2.459 eV	0.746 eV	1.577 eV
	542.50 nm	1556 nm	504.1 nm	1663 nm	786.4 nm
	f = 1.3452	f = 0.0015	f = 0.909	f = 0.001	f = 0.148
4d	2.241 eV	0.771 eV	2.372 eV	0.679 eV	1.440 eV
	553.15 nm	1608 nm	522.6 nm	1825 nm	861.1 nm
	f = 1.2159	f = 0.0020	f = 0.6892	f = 0.002	f = 0.091

However, the minimum energy of the excited 8U-Rhs, like in the case of MG[39] (but different from planar RB), corresponds to the structure with rotated lateral rings. This structure is characterized by low energy transitions to the ground state with extremely low oscillator strengths (Tables 3 and S1). Such type of structure is created in the evolution of the system after electronic excitation, during which the rotation of phenyl rings is accompanied by intramolecular CT. A similar mechanism has been proposed for MG.[39] To gain further insights, we have extended our calculations to include R^+Cl^- ion pairs. The reason for this lies in that the calculation results of RB[42] show that the three orbitals of Cl^- are energetically neighbor to the HOMO orbital located on R^+. This also applies for the urea-bridged rhodamines in solvents of medium polarity (Figure S5). With such an energy arrangement of R^+Cl^- system orbitals, the appearance of intermolecular CT states (HOMO(Cl^-) → LUMO(R^+)) located near states localized on 8U-Rhs can be expected.

The simulation of absorption spectra of the ion pair R^+Cl^- of **4b** (Table S3) illustrates that in low- and medium-polarity solvents, weak intensity CT transitions are present, but they are hidden under the large intensity band for the $S_0 \rightarrow S_1$ transition localized on 8U-Rh^+. This leads to subtle changes in the absorption spectrum, including peak broadening and a small shift of the main absorption band. Such effects disappear in polar solvents.

Optimization of the R^+Cl^- pair in the excited state showed that, in addition to the previously described structure with rotated lateral rings (A-case, similar to MG), a minimum of another type appears (B-case) (Table S4). This corresponds to a molecule with less twisted rings and is described by an intermolecular CT configuration because the HOMO orbital is predominately located on Cl^- (Table S4). The energies and oscillator strengths of the $S_1 \rightarrow S_0$ transition corresponding to the B-structure are greater in comparison to the A-structure (Table 3). Comparing three optimized ion pair structures, it can be stated that the B-structure is characterized by the smallest distance between R^+ and Cl^- (Table S4, Figure 4), allowing for

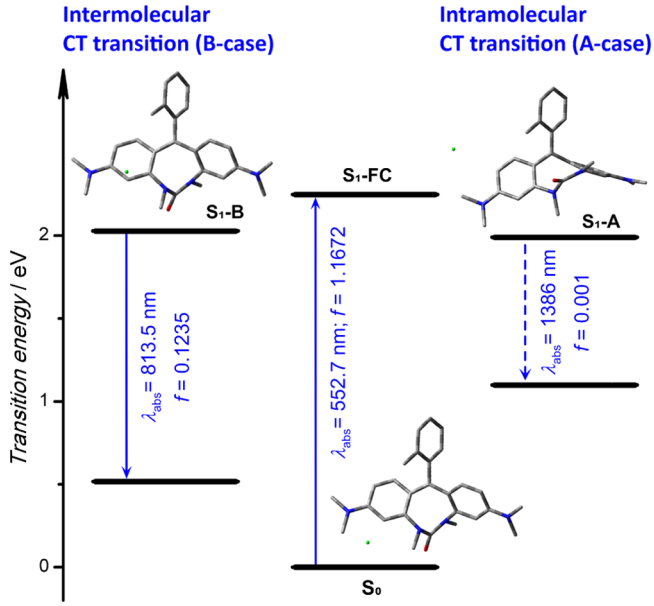

Figure 4. Diagram of electronic states of **4b** as an ion pair R^+Cl^- optimized by B3LYP and TD B3LYP/6-31G(d,p) methods in acetonitrile solution. Three structures are shown: S_0 optimized in the ground state and both A and B optimized in the excited state.

more efficient mixing of electronic configurations. In other cases, that is, forms of S_0 and A, the presence of Cl^- in solution plays a smaller role, and their properties are described well enough by analyzing their cations.

However, it should be noted that with such complex systems as 8U-Rhs, full mapping of the potential energy surface in the excited state is a very difficult task. In Table S4, we indicate this problem by providing two sets of values for each of the optimized structures obtained using different starting points in space. It can be assumed that there are even more possible positions, and the experimental results are because of an average of the ensemble.

Figure 4 presents a diagram of electronic states for compound **4b** as a R^+Cl^- pair in acetonitrile solution (data in Table 3).

https://dx.doi.org/10.1021/acs.joc.0c00414
J. Org. Chem. 2020, 85, 5973−5980

Upon excitation, the 8U-Rhs can relax from the S_1 state into a practically dark form A with a very low energy gap to the ground state (0.7−1.1 eV with B3LYP calculations and larger by about 0.4 eV with the CAM-B3LYP method) and with the oscillator strength value close to zero (Tables 3 and S4). This is the pathway of nonradiative decay that has been analyzed in detail for MG.[37−39] In this form of excited state, the lateral ring planes of the 8U-Rhs are significantly twisted with respect to each other, which is possible because of the flexibility of the eight-membered ring.

CONCLUSIONS

In summary, we have designed and synthesized a series of rhodamine analogues bearing a central eight-membered ring. These new dyes adopt a curved geometry in the crystal lattice because of the highly strained central ring. In terms of electronic absorption behavior, 8U-Rhs resemble both rhodamines and triphenylmethane dyes. The 8U-Rhs exhibit strong absorption, which is red-shifted with respect to conventional rhodamine dyes and blue-shifted compared to MG that lacks a central electron-donating group and has free rotation for all phenyl groups. The presence of the central eight-membered ring in the 8U-Rhs causes quenching of fluorescence in all nonviscous solvents because of nonradiative deactivation pathways, in a similar manner to MG. Weak 8U-Rhs' fluorescence can be attributed to the CT transition with small oscillator strength in the R^+Cl^- ion pair. In such a pair (contact in solution), there is a relatively short distance between Cl and R, and intermolecular CT interactions are factors that compete with the tendency to rotate the lateral rings. Although in this work this intermolecular CT mechanism is considered as a source of observed weak fluorescence, it can also be seen as a mechanism that quenches the fluorescence of the chromophore that is excited as a high-oscillator system. In this context, it can be thought that the concentration quenching of RB fluorescence,[43] which is discussed in terms of dimer formation, may also be associated with the formation of CT contact pairs.

EXPERIMENTAL SECTION

All chemicals were used as received unless otherwise noted. All reported ^{1}H NMR spectra were collected using 500 and 600 MHz spectrometers. Chemical shifts (δ ppm) were determined with TMS as the internal reference; J values are given in Hz. Chromatography was performed on silica gel (230−400 mesh). The mass spectra were obtained by electron ionization (EI-MS) or electrospray ionization (ESI-MS). All photophysical studies were performed with freshly-prepared air-equilibrated solutions at room temperature (298 K).

A PerkinElmer Lambda 25 UV/Vis spectrophotometer and a Hitachi F7000 fluorescence spectrometer were used to acquire the absorption and emission spectra. Spectroscopic grade solvents were used without further purification. Fluorescence quantum yields were determined in CH_2Cl_2, acetonitrile, and water using sulforhodamine 101 in ethanol as the standard. The solid-state fluorescence measurements were conducted using a 405 nm diode laser coupled with a 540 nm longpass filter.

Preparation of SOA Solutions for Measurements. Concentrated dye solutions in dichloroethane are added to a homogeneous mixture of SOA and dichloroethane in a 9:1 ratio (small amount of dichloroethane makes the mixture less viscous). A homogenous dye solution is concentrated at reduced pressures and viscous foam-like dye solution in SOA was additionally dried in high-vacuum for several hours. The flask with the SOA solution was immersed in an oil bath (100−110 °C), and as soon as it became liquid it is rapidly transferred into the cuvette. To get rid of air bubbles, the cuvette was put into a round-bottom flask and the flask was immersed in the oil bath for several minutes. After cooling, the cuvette with the sample is ready for measurements.

Preparation of Ground Powder for Measurements. The samples were prepared either in a polycrystalline form or as ground powder. The quantum yields in the solid states were measured using an Edinburgh FLS980 fluorimeter equipped with an integrating sphere assembly F-M01.

General Procedure for the Preparation of Compounds ***2***. An ethanol solution (20 mL) of 6 mmol *N*,*N*,*N*-trimethyl-*m*-phenylenediamine **1** (or *N*-methyl-3-(pyrrolidin-1-yl)aniline **5**) and an aromatic aldehyde (3 mmol) containing two drops of acetic acid was stirred for 48 h at r.t. The product was filtered off, washed with ethanol, and dried in vacuo to give a pure product.

4,4′-((4-Chlorophenyl)methylene)bis(N^1,N^1,N^3-trimethylbenzene-1,3-diamine) ***2a***. Off-white crystalline solid. Yield 78% (0.99 g). ^{1}H NMR (500 MHz, DMSO-d_6): δ 7.25 (d, 2H, J = 8.5 Hz), 6.94 (d, 2H, J = 8.4 Hz), 6.25 (d, 2H, J = 8.3 Hz), 5.86−5.89 (m, 4H), 5.22 (s, 1H), 4.39 (q, 2H, J = 4.8 Hz), 2.80 (s, 12H), 2.61 (d, 6H, J = 5.0 Hz); ^{13}C NMR (126 MHz, DMSO-d_6): δ 150.7, 147.7, 143.4, 131.4, 130.7, 129.6, 128.2, 116.3, 101.2, 95.5, 42.9, 40.7, 30.8; HRMS (ESI-TOF) m/z: $[M + H]^+$ calcd for $C_{25}H_{32}N_4Cl$, 423.2315; found, 423.2299.

4,4′-((2-Methylphenyl)methylene)bis(N^1,N^1,N^3-trimethylbenzene-1,3-diamine) ***2b***. Off-white crystalline solid. Yield 79% (0.95 g). It is not possible to get clean NMR spectra, though both MS spectral and elemental analyses suggest product **2b**.

Elemental analysis: calcd for $C_{26}H_{34}N_4$: C, (77.57%); H, (8.51%); N, (13.92%). Found: C, (77.60%); H, (8.47%); N, (13.81%); HRMS (EI-magnetic sector) m/z: $[M]^{+\bullet}$ calcd for $C_{26}H_{34}N_4$, 402.2783; found, 402.2787.

4,4′-((2,4,6-Trimethylphenyl)methylene)bis(N^1,N^1,N^3-trimethylbenzene-1,3-diamine) ***2c***. Off-white crystalline solid. Yield 44% (0.56 g). ^{1}H NMR (500 MHz, DMSO-d_6): δ 6.77 (s, 2H), 6.33 (d, 2H, J = 9.0 Hz), 5.92−5.94 (m, 4H), 5.16 (s, 1H), 3.67 (s, 2H), 2.85 (s, 12H), 2.63 (d, 6H, J = 5.0 Hz), 2.20 (s, 3H), 18.7 (s, 6H); ^{13}C NMR (126 MHz, DMSO-d_6): δ 150.7, 148.2, 137.4, 135.9, 135.2, 130.6, 129.4, 114.6, 101.6, 95.3, 41.8, 40.7, 31.0, 21.7, 20.8; HRMS (EI-magnetic sector) m/z: $[M]^{+\bullet}$ calcd for $C_{28}H_{38}N_4$, 430.3096; found, 430.3094.

4,4′-((2-(Trifluoromethyl)phenyl)methylene)bis(N^1,N^1,N^3-trimethylbenzene-1,3-diamine) ***2d***. Off-white crystalline solid. Yield 63% (0.86 g). ^{1}H NMR (500 MHz, DMSO-d_6): δ 7.69 (d, 1H, J = 7.6 Hz), 7.53 (t, 1H, J = 7.7 Hz), 7.42 (t, 1H, J = 7.6 Hz), 7.01 (d, 1H, J = 7.8 Hz), 6.20 (d, 2H, J = 8.8 Hz), 5.90−5.91 (m, 4H), 5.39 (s, 1H), 4.09 (q, 2H, J = 4.8 Hz), 2.84 (s, 12H), 2.62 (d, 6H, J = 5.0 Hz); ^{13}C NMR (126 MHz, DMSO-d_6): δ 150.7, 147.5, 142.7, 132.3, 131.4, 129.4, 127.2, 115.8, 101.1, 95.7, 40.6, 30.9; ^{19}F NMR (470 MHz, DMSO-d_6): δ −58.18; HRMS (EI-magnetic sector) m/z: $[M]^{+\bullet}$ calcd for $C_{26}H_{31}F_3N_4$, 456.2501; found, 456.2508.

6,6′-((2-Methylphenyl)methylene)bis(N-methyl-3-(pyrrolidin-1-yl)aniline) ***2e***. Off-white crystalline solid. Yield 80% (1.09 g). ^{1}H NMR (500 MHz, DMSO-d_6): δ 7.03−7.09 (m, 2H), 7.00 (t, 1H, J = 6.8 Hz), 6.64 (d, 1H, J = 7.7 Hz), 6.21 (d, 2H, J = 8.1 Hz), 5.70−5.74 (m, 4H), 5.13 (s, 1H), 4.19 (q, 2H, J = 4.3 Hz), 3.16−3.18 (m, 8H), 2.63 (d, 6H, J = 5.0 Hz), 2.05 (s, 3H), 1.89−1.91 (m, 8H); ^{13}C NMR (126 MHz, DMSO-d_6): δ 147.9, 147.8, 142.8, 137.3, 130.5, 129.6, 128.2, 126.2, 125.6, 114.9, 100.4, 94.6, 47.7, 30.9, 25.4, 19.5; HRMS (EI-magnetic sector) m/z: $[M]^{+\bullet}$ calcd for $C_{30}H_{38}N_4$, 454.3096; found, 454.3104.

N-Methyl-3-(pyrrolidin-1-yl)aniline ***5***.[44] A mixture containing 4.07 g (0.018 mol) of 1-(3-bromophenyl)pyrrolidine, 22.7 mL of 41% (0.27 mol) methylamine water solution, and 0.057 g (0.65 mmol) of copper powder was heated at 100 °C in a pressure flask for 6 days with stirring. Upon cooling, the reactant was filtered through the cotton pad and the product was extracted with ethyl acetate. The organic layer was dried over $MgSO_4$. The inorganic material was filtered off and the filtrate was evaporated. The product was purified by distillation at 100−103 °C under reduced pressure (0.15 mbar), and the pure product crystallized as an off-white solid. Yield 2.00 g (63%). ^{1}H NMR (500 MHz, $CDCl_3$): δ 7.05 (t, 1H, J = 8.0 Hz), 5.99−6.01 (m, 2H), 5.83 (t, 1H, J = 2.1 Hz), 3.63 (br s, 1H), 3.26−3.28 (m, 4H), 2.83 (s, 3H), 1.96−1.98 (m, 4H); ^{13}C NMR (126 MHz, $CDCl_3$): δ 150.4, 149.1, 129.8, 101.9, 100.9, 95.8,

https://dx.doi.org/10.1021/acs.joc.0c00414
J. Org. Chem. 2020, 85, 5973−5980

47.6, 30.9, 25.4; HRMS (EI-magnetic sector) m/z: $[M]^{+\bullet}$ calcd for $C_{11}H_{16}N_2$, 176.1313; found, 176.1317.

General Procedure for the Preparation of Compounds ***3***. A solution of compound **2** (2 mmol) and diisopropylethylamine (6 mmol) in dry CH_2Cl_2 (20 mL) was cooled to −5 °C under an argon atmosphere. Triphosgene (1 mmol) was added to the stirred solution in one portion. The solution was stirred for 30 min at 0 °C. The solution was stirred at r.t. for an additional period of time individually for each product. On reaction completion, the solution was diluted with 100 mL of CH_2Cl_2 and washed with water. The organic layer was dried over $MgSO_4$. Upon evaporation, the residue was purified by column chromatography (SiO_2, toluene/ethyl acetate 1:1). After evaporation of the product fraction, the product was dried at 140 °C for 1 h.

12-(4-Chlorophenyl)-3,9-bis(dimethylamino)-5,7-dimethyl-7,12-dihydrodibenzo[d,g][1,3]diazocin-6(5H)-one ***3a***. Reaction time: 3 days. Column chromatography (SiO_2, toluene/ethyl acetate 1:1). Off-white crystalline solid. Yield 53% (0.48 g). ^{1}H NMR (500 MHz, DMSO-d_6): δ 7.21 (d, 2H, J = 8.5 Hz), 7.11 (d, 2H, J = 8.5 Hz), 6.67 (d, 2H, J = 8.3 Hz), 6.52 (dd, 2H, J = 8.4 Hz, J = 2.5 Hz), 6.44 (d, 2H, J = 2.5 Hz), 5.34 (s, 1H), 2.88 (s, 12H), 2.38 (s, 6H); ^{13}C NMR (126 MHz, DMSO-d_6): δ 162.5, 153.5, 147.4, 135.5, 132.9, 131.9, 130.5, 124.4, 111.9, 108.7, 56.3, 43.2, 39.0; HRMS (EI-magnetic sector) m/z: $[M]^{+\bullet}$ calcd for $C_{26}H_{29}N_4OCl$, 448.2030; found, 448.2021.

3,9-Bis(dimethylamino)-12-(4-methylphenyl)-5,7-dimethyl-7,12-dihydrodibenzo[d,g][1,3]diazocin-6(5H)-one ***3b***. Reaction time: 4 days. Column chromatography (SiO_2, toluene/ethyl acetate 1:1). Off-white crystalline solid. Yield 30% (0.26 g). ^{1}H NMR (500 MHz, $CDCl_3$): δ 7.15 (d, 2H, J = 8.4 Hz), 7.09 (t, 1H, J = 7.4 Hz), 6.97−7.03 (m, 2H), 6.70 (d, 1H, J = 7.5 Hz), 6.54 (d, 2H, J = 9.3 Hz), 6.40 (s, 2H), 5.32 (s, 1H), 2.94 (s, 12H), 2.48 (s, 6H), 1.98 (s, 3H); ^{13}C NMR (126 MHz, $CDCl_3$): δ 160.2, 150.3, 144.6, 142.5, 135.5, 132.8, 130.2, 129.3, 125.79, 125.76, 122.4, 109.5, 105.5, 54.5, 40.6, 36.0, 20.8; HRMS (EI-magnetic sector) m/z: $[M]^{+\bullet}$ calcd for $C_{27}H_{32}N_4O$, 428.2576; found, 428.2567.

3,9-Bis(dimethylamino)-12-(2,4,6-trimethylphenyl)-5,7-dimethyl-7,12-dihydrodibenzo[d,g][1,3]diazocin-6(5H)-one ***3c***. Reaction time: 14 days. Column chromatography (SiO_2, toluene/ethyl acetate 1:1). Off-white crystalline solid. Yield 57% (0.52 g). ^{1}H NMR (500 MHz, $CDCl_3$): δ 6.88 (s, 2H), 6.74 (d, 2H, J = 8.8 Hz), 6.53 (s, 2H), 6.39 (d, 2H, J = 9.7 Hz), 5.85 (s, 1H), 3.05 (s, 3H), 2.90 (s, 12H), 2.30 (s, 3H), 2.04 (s, 6H); ^{13}C NMR (126 MHz, $CDCl_3$): δ 163.4, 149.3, 145.5, 138.7, 137.4, 135.4, 130.9, 129.9, 124.0, 109.9, 106.2, 43.9, 40.5, 36.5, 22.1, 20.8; HRMS (ESI-TOF) m/z: $[M + H]^+$ calcd for $C_{29}H_{36}N_4O$, 457.2967; found, 457.2967.

3,9-Bis(dimethylamino)-12-(2-(trifluoromethyl)phenyl)-5,7-dimethyl-7,12-dihydrodibenzo[d,g][1,3]diazocin-6(5H)-one ***3d***. Reaction time: 18 days. Column chromatography (SiO_2, toluene/ethyl acetate 1:1). Off-white crystalline solid. Yield 30% (0.29 g). ^{1}H NMR (500 MHz, $CDCl_3$): δ 7.58 (d, 1H, J = 8.4 Hz), 7.43 (t, 1H, J = 8.2 Hz), 7.24 (t, 1H, J = 7.4 Hz), 7.11 (d, 2H, J = 9.1 Hz), 6.99 (d, 1H, J = 7.9 Hz), 6.52 (d, 2H, J = 6.7 Hz), 2.94 (s, 12H), 2.51 (s, 6 H); ^{13}C NMR (126 MHz, $CDCl_3$): δ 160.2, 150.5, 144.6, 132.6, 132.7, 131.9, 131.5, 126.5, 126.4, 125.9, 109.4, 105.3, 52.4, 40.6, 36.1; ^{19}F NMR (470 MHz, $CDCl_3$): δ −58.77; HRMS (EI-magnetic sector) m/z: $[M]^{+\bullet}$ calcd for $C_{27}H_{29}F_3N_4O$, 482.2293; found, 482.2288.

5,7-Dimethyl-3,9-di(pyrrolidin-1-yl)-12-(2-methylphenyl)-7,12-dihydrodibenzo[d,g][1,3]diazocin-6(5H)-one ***3e***. Reaction time: 11 days. Column chromatography (SiO_2, toluene/ethyl acetate 1:1). Off-white crystalline solid. Yield 56% (0.54 g). ^{1}H NMR (500 MHz, $CDCl_3$): δ 7.41 (d, 1H, J = 7.9 Hz), 7.30 (d, 2H, J = 8.3 Hz), 7.24 (t, 1H, J = 7.3 Hz), 7.03−7.10 (m, 2H), 6.45 (dd, 2H, J = 8.3 Hz, J = 2.3 Hz), 6.40 (d, 2H, J = 2.0 Hz), 5.63 (s, 1H), 2.99−3.02 (m, 8H), 2.77 (s, 6H), 2.19 (s, 3H), 1.59−1.61 (m, 8H); ^{13}C NMR (126 MHz, $CDCl_3$): δ 160.0, 147.7, 145.3, 143.4, 133.0, 130.1, 130.0, 127.9, 127.7, 127.6, 126.0, 125.7, 108.6, 104.6, 55.3, 47.2, 35.9, 25.1, 20.7; HRMS (EI-magnetic sector) m/z: $[M]^{+\bullet}$ calcd for $C_{31}H_{36}N_4O$, 480.2889; found, 480.2894.

General Procedure for Oxidation of Compounds ***3*** *to Rhodamine Analogues* ***4***. In a 50 mL round bottom flask, 1 mmol cyclic compound **3a**−**e** and 1.1 mmol DDQ were dissolved in 12 mL of dry DCM. The resulting solution was stirred for 30 min at room temperature under an argon atmosphere. The reaction mixture was then evaporated and the residue was purified by column chromatography (silica) using a solvent system of 9:1 CH_2Cl_2/MeOH with the addition of 1.2 g of Aliquat 336 (trioctylmethylammonium chloride) for each 100 mL of eluent. After evaporation of the solvents, hexane was added to the mixture. The product was filtered off, washed with fresh hexane, and dried at 80 °C for 4 h (**4d** at 40 °C). In some cases, when the crystalline product was contaminated with the residue of Aliquat 336, the product was dissolved with a small amount of DCM and crystallized by the addition of diethyl ether and a few drops of methanol to give a pure reaction product.

(Z)-N-(12-(4-Chlorophenyl)-9-(dimethylamino)-5,7-dimethyl-6-oxo-6,7-dihydrodibenzo[d,g][1,3]diazocin-3(5H)-ylidene)-N-methylmethanaminium Chloride ***4a***. Dark glossy crystalline solid. Column chromatography (SiO_2) was performed using a solvent system of 9:1 CH_2Cl_2/MeOH with the addition of 1.2 g of Aliquat 336. Yield 70% (0.34 g). ^{1}H NMR (500 MHz, $CDCl_3$): δ 7.47 (d, 2H, J = 8.4 Hz), 7.05 (d, 2H, J = 8.4 Hz), 6.87 (d, 2H, J = 9.6 Hz), 6.73 (dd, 2H, J = 9.6 Hz, J = 2.5 Hz), 6.51 (d, 2H, J = 2.5 Hz), 3.38 (s, 12H), 3.22 (s, 6H); ^{13}C NMR (126 MHz, $CDCl_3$): δ 162.2, 161.0, 157.1, 153.4, 141.1, 139.4, 137.6, 134.3, 128.6, 125.0, 112.5, 103.1, 41.4, 37.3; HRMS (ESI-TOF) m/z: $[M]^+$ calcd for $C_{26}H_{28}N_4OCl^+$, 447.1952; found, 447.1970.

(Z)-N-(9-(Dimethylamino)-5,7-dimethyl-6-oxo-12-(2-methylphenyl)-6,7-dihydrodibenzo[d,g][1,3]diazocin-3(5H)-ylidene)-N-methylmethanaminium Chloride ***4b***. Dark glossy crystalline solid. Column chromatography (SiO_2) was performed using a solvent system of 9:1 CH_2Cl_2/MeOH with the addition of 1.2 g of Aliquat 336. Yield 65% (0.30 g). ^{1}H NMR (500 MHz, $CDCl_3$): δ 7.44 (t, 1H, J = 8.0 Hz), 7.32 (d, 1H, 7.5 Hz), 7.29 (d, 1H, J = 7.5 Hz), 6.90−6.93 (m, 2H), 6.78 (d, 1H, J = 9.4 Hz), 6.74 (dd, 1H, J = 9.7 Hz, J = 2.4 Hz), 6.61 (dd, 1H, J = 9.5 Hz, J = 2.5 Hz), 6.53 (dd, 2H, J = 16.1 Hz, J = 2.4 Hz), 3.45 (s, 6H), 3.30 (s, 6H), 3.27 (s, 3H), 3.21 (s, 3H), 1.87 (s, 3H); ^{13}C NMR (126 MHz, $CDCl_3$): δ 164.0, 160.9, 158.3, 155.8, 155.2, 151.1, 142.0, 140.2, 137.7, 137.0, 131.8, 130.9, 130.3, 125.7, 125.7, 124.4, 112.8, 112.1, 103.7, 102.6, 41.7, 40.9, 37.27, 37.25, 19.7; HRMS (ESI-TOF) m/z: $[M]^+$ calcd for $C_{27}H_{31}N_4O^+$, 427.2498; found, 427.2499.

(Z)-N-(9-(Dimethylamino)-5,7-dimethyl-6-oxo-12-(2,4,6-trimethylphenyl)-6,7-dihydrodibenzo[d,g][1,3]diazocin-3(5H)-ylidene)-N-methylmethanaminium Chloride ***4c***. Dark glossy crystalline solid. Column chromatography (SiO_2) was performed using a solvent system of 9:1 CH_2Cl_2/MeOH with the addition of 1.2 g of Aliquat 336. Yield 85% (0.42 g). ^{1}H NMR (500 MHz, $CDCl_3$): δ 6.92 (s, 2H), 6.85 (d, 2H, J = 9.6 Hz), 6.65 (dd, 2H, J = 9.6 Hz, J = 2.5 Hz), 6.48 (d, 2H, J = 2.5 Hz), 5.28 (s, 1H), 3.35 (s, 12H), 3.19 (s, 6H), 2.33 (s, 3H), 1.76 (s, 6H); ^{13}C NMR (126 MHz, $CDCl_3$): δ 167.0, 163.8, 159.7, 155.8, 142.5, 141.7, 141.0, 138.7, 131.7, 127.5, 115.4, 105.9, 43.9, 40.0, 23.8, 22.5; HRMS (ESI-TOF) m/z: $[M]^+$ calcd for $C_{29}H_{35}N_4O^+$, 455.2811; found, 455.2807.

(Z)-N-(9-(Dimethylamino)-5,7-dimethyl-6-oxo-12-(2-(trifluoromethyl)phenyl)-6,7-dihydrodibenzo[d,g][1,3]diazocin-3(5H)-ylidene)-N-methylmethanaminium Chloride ***4d***. Dark glossy crystalline solid. Column chromatography (SiO_2) was performed using a solvent system of 9:1 CH_2Cl_2/MeOH with the addition of 1.2 g of Aliquat 336. Yield 5% (26 mg). ^{1}H NMR (500 MHz, $CDCl_3$): δ 7.77−7.78 (m, 2H), 7.67 (t, 1H, J = 7.8 Hz), 7.25 (d, 1H, J = 5.5 Hz), 6.89 (d, 1H, J = 10.0 Hz), 6.78 (dd, 1H, J = 10.0 Hz, J = 2.2 Hz), 6.58−6.60 (m, 1H), 6.50 (m, 2H), 6.45 (d, 1H, J = 2.0 Hz), 3.56 (s, 6H), 3.29 (s, 3H), 3.18 (s, 3H), 3.17 (s, 6H); ^{13}C NMR (126 MHz, $CDCl_3$): δ 160.1, 159.6, 159.2, 157.8, 154.3, 148.5, 148.5, 140.6, 139.9, 136.3, 134.0, 132.1, 130.1, 127.0, 126.9, 122.9, 114.2, 111.1, 105.0, 101.3, 42.4, 40.4, 37.1; ^{19}F NMR (470 MHz, $CDCl_3$): δ −58.31; HRMS (ESI-TOF) m/z: $[M]^+$ calcd for $C_{27}H_{28}F_3N_4O^+$, 481.2202; found, 481.2213.

(Z)-1-(5,7-Dimethyl-6-oxo-9-(pyrrolidin-1-yl)-12-(2-methylphenyl)-6,7-dihydrodibenzo[d,g][1,3]diazocin-3(5H)-ylidene)pyrrolidin-1-ium Chloride ***4e***. The reaction did not reach a full conversion in 2.5 h. Column chromatography (SiO_2) was performed using a solvent system of 9:1 CH_2Cl_2/MeOH with the addition of 1.2 g of Aliquat 336. After purification, the product was contaminated with Aliquat 336. The product was recrystallized from the mixture of CH_2Cl_2 and diethyl ether as a dark glossy crystalline solid. Yield 14% (0.07 g). ^{1}H NMR (500

https://dx.doi.org/10.1021/acs.joc.0c00414
J. Org. Chem. 2020, 85, 5973−5980

MHz, $CDCl_3$): δ 7.43 (t, 1H, J = 7.3 Hz), 7.28−7.32 (m, 2H), 6.89−6.94 (m, 2H), 6.77 (d, 1H, J = 9.3 Hz), 6.61 (d, 1H, J = 7.9 Hz), 6.49 (d, 1H, J = 9.4 Hz), 6.42 (s, 2H), 3.57−3.80 (br s, 8H), 3.26 (s, 3H), 3.21 (s, 3H), 2.15−2.18 (m, 8H), 1.88 (s, 3H); ^{13}C NMR (126 MHz, $CDCl_3$): δ 163.8, 161.2, 155.6, 155.1, 153.2, 151.0, 142.2, 140.2, 137.8, 137.0, 131.9, 130.8, 130.2, 125.8, 125.7, 124.5, 113.6, 112.7, 104.2, 103.4, 49.8, 48.9, 37.2, 25.3, 25.2, 19.7; HRMS (ESI-TOF) m/z: $[M]^+$ calcd for $C_{31}H_{35}N_4O^+$, 479.2811; found, 479.2815.

Preparation of Single Crystals. Monocrystalline samples were obtained by the vapor diffusion method using acetonitrile (solvent) and diethyl ether (precipitant) for compound **4b** and acetonitrile (solvent) and THF (precipitant) for **4c**.

■ ASSOCIATED CONTENT

Supporting Information

The Supporting Information is available free of charge at https://pubs.acs.org/doi/10.1021/acs.joc.0c00414.

Experimental details, spectral data for all products, and X-ray structure (PDF)
(CIF)
(CIF)

■ AUTHOR INFORMATION

Corresponding Authors

Pi-Tai Chou − *Department of Chemistry, National Taiwan University, 10617 Taipei, Taiwan;* orcid.org/0000-0002-8925-7747; Email: chop@ntu.edu.tw

Irena Deperasińska − *Institute of Physics Polish Academy of Sciences, 02-668 Warsaw, Poland*; Email: deper@ifpan.edu.pl

Daniel T. Gryko − *Institute of Organic Chemistry, Polish Academy of Sciences, 01-224 Warsaw, Poland;* orcid.org/0000-0002-2146-1282; Email: dtgryko@icho.edu.pl

Authors

Yevgen M. Poronik − *Institute of Organic Chemistry, Polish Academy of Sciences, 01-224 Warsaw, Poland*

Filip Ambicki − *Institute of Organic Chemistry, Polish Academy of Sciences, 01-224 Warsaw, Poland*

Sheng-Ming Tseng − *Department of Chemistry, National Taiwan University, 10617 Taipei, Taiwan*

Complete contact information is available at: https://pubs.acs.org/10.1021/acs.joc.0c00414

Author Contributions

The manuscript was written with contributions from all authors.

Notes

The authors declare no competing financial interest.

■ ACKNOWLEDGMENTS

The authors would like to thank the Foundation for Polish Science (TEAM POIR.04.04.00-00-3CF4/16-00) and Global Research Laboratory Program (2014K1A1A2064569) through the National Research Foundation (NRF) funded by the Ministry of Science, ICT & Future Planning (Korea). We thank Dr. David C. Young for amending the manuscript. Theoretical calculations were performed at the Interdisciplinary Centre of Mathematical and Computer Modelling (ICM) of the Warsaw University under the computational grant no. G-32-10.

■ REFERENCES

(1) *Molecular Probes Handbook, A Guide to Fluorescent Probes and Labeling Technologies*, 11th ed.; Johnson, I., Spence, M. T. Z., Eds.; Life Technologies Corporation, 2010.

(2) Yamagami, A.; Ishimura, H.; Katori, A.; Kuramochi, K.; Tsubaki, K. Syntheses and Properties of the V-Shaped Dimeric Xanthene Dyes. *Org. Biomol. Chem.* **2016**, *14*, 10963−10972.

(3) Rosenberg, M.; Santella, M.; Bogh, S. A.; Muñoz, A. V.; Andersen, H. O. B.; Hammerich, O.; Bora, I.; Lincke, K.; Laursen, B. W. Extended Triangulenium Ions: Syntheses and Characterization of Benzo-Bridged Dioxa- and Diazatriangulenium Dyes. *J. Org. Chem.* **2019**, *84*, 2556−2567.

(4) Yang, Y.; Lowry, M.; Xu, X.; Escobedo, J. O.; Sibrian-Vazquez, M.; Wong, L.; Schowalter, C. M.; Jensen, T. J.; Fronczek, F. R.; Warner, I. M.; et al. Seminaphthofluorones Are a Family of Water-Soluble, Low Molecular Weight, NIR-Emitting Fluorophores. *Proc. Natl. Acad. Sci. U.S.A.* **2008**, *105*, 8829−8834.

(5) Wang, L. G.; Munhenzva, I.; Sibrian-Vazquez, M.; Escobedo, J. O.; Kitts, C. H.; Fronczek, F. R.; Strongin, R. M. Altering Fundamental Trends in the Emission of Xanthene Dyes. *J. Org. Chem.* **2019**, *84*, 2585−2595.

(6) Katori, A.; Azuma, E.; Ishimura, H.; Kuramochi, K.; Tsubaki, K. Fluorescent Dyes with Directly Connected Xanthone and Xanthene Units. *J. Org. Chem.* **2015**, *80*, 4603−4610.

(7) Shieh, P.; Dien, V. T.; Beahm, B. J.; Castellano, J. M.; Wyss-Coray, T.; Bertozzi, C. R. CalFluors: A Universal Motif for Fluorogenic Azide Probes across the Visible Spectrum. *J. Am. Chem. Soc.* **2015**, *137*, 7145−7151.

(8) Lukinavičius, G.; Reymond, L.; Umezawa, K.; Sallin, O.; D'Este, E.; Göttfert, F.; Ta, H.; Hell, S. W.; Urano, Y.; Johnsson, K. Fluorogenic Probes for Multicolor Imaging in Living Cells. *J. Am. Chem. Soc.* **2016**, *138*, 9365−9368.

(9) Ikeno, T.; Nagano, T.; Hanaoka, K. Silicon-Substituted Xanthene Dyes and Their Unique Photophysical Properties for Fluorescent Probes. *Chem.—Asian J.* **2017**, *12*, 1435−1446.

(10) Grzybowski, M.; Taki, M.; Yamaguchi, S. Selective Conversion of P=O-Bridged Rhodamines into P=O-Rhodols: Solvatochromic Near-Infrared Fluorophores. *Chem.—Eur. J.* **2017**, *23*, 13028−13032.

(11) Liu, J.; Sun, Y.-Q.; Zhang, H.; Shi, H.; Shi, Y.; Guo, W. Sulfone-Rhodamines: A New Class of near-Infrared Fluorescent Dyes for Bioimaging. *ACS Appl. Mater. Interfaces* **2016**, *8*, 22953−22962.

(12) Butkevich, A. N.; Mitronova, G. Y.; Sidenstein, S. C.; Klocke, J. L.; Kamin, D.; Meineke, D. N. H.; D'Este, E.; Kraemer, P.-T.; Danzl, J. G.; Belov, V. N.; et al. Fluorescent Rhodamines and Fluorogenic Carbopyronines for Super-Resolution STED Microscopy in Living Cells. *Angew. Chem., Int. Ed.* **2016**, *55*, 3290−3294.

(13) Grimm, J. B.; Sung, A. J.; Legant, W. R.; Hulamm, P.; Matlosz, S. M.; Betzig, E.; Lavis, L. D. Carbofluoresceins and Carborhodamines as Scaffolds for High-Contrast Fluorogenic Probes. *ACS Chem. Biol.* **2013**, *8*, 1303−1310.

(14) Sednev, M. V.; Wurm, C. A.; Belov, V. N.; Hell, S. W. Carborhodol: A New Hybrid Fluorophore Obtained by Combination of Fluorescein and Carbopyronine Dye Cores. *Bioconjugate Chem.* **2013**, *24*, 690−700.

(15) Takahashi, S.; Kagami, Y.; Hanaoka, K.; Terai, T.; Komatsu, T.; Ueno, T.; Uchiyama, M.; Koyama-Honda, I.; Mizushima, N.; Taguchi, T.; et al. Development of a Series of Practical Fluorescent Chemical Tools to Measure PH Values in Living Samples. *J. Am. Chem. Soc.* **2018**, *140*, 5925−5933.

(16) Lavis, L. D. Chemistry Is Dead. Long Live Chemistry! *Biochemistry* **2017**, *56*, 5165−5170.

(17) Gong, Y.-J.; Zhang, X.-B.; Mao, G.-J.; Su, L.; Meng, H.-M.; Tan, W.; Feng, S.; Zhang, G. A Unique Approach toward Near-Infrared Fluorescent Probes for Bioimaging with Remarkably Enhanced Contrast. *Chem. Sci.* **2016**, *7*, 2275−2285.

(18) Chan, J.; Dodani, S. C.; Chang, C. J. Reaction-Based Small-Molecule Fluorescent Probes for Chemoselective Bioimaging. *Nat. Chem.* **2012**, *4*, 973−984.

(19) Deo, C.; Sheu, S.-H.; Seo, J.; Clapham, D. E.; Lavis, L. D. Isomeric Tuning Yields Bright and Targetable Red Ca2+ Indicators. *J. Am. Chem. Soc.* **2019**, *141*, 13734−13738.

(20) Shieh, P.; Hangauer, M. J.; Bertozzi, C. R. Fluorogenic Azidofluoresceins for Biological Imaging. *J. Am. Chem. Soc.* **2012**, *134*, 17428−17431.
(21) Poronik, Y. M.; Vygranenko, K. V.; Gryko, D.; Gryko, D. T. Rhodols − Synthesis, Photophysical Properties and Applications as Fluorescent Probes. *Chem. Soc. Rev.* **2019**, *48*, 5242−5265.
(22) García, R.; Herranz, M. Á.; Torres, M. R.; Bouit, P.-A.; Delgado, J. L.; Calbo, J.; Viruela, P. M.; Ortí, E.; Martín, N. Tuning the Electronic Properties of Nonplanar ExTTF-Based Pusha-Pull Chromophores by Aryl Substitution. *J. Org. Chem.* **2012**, *77*, 10707−10717.
(23) Kato, S.-i.; Diederich, F. Non-Planar Push-Pull Chromophores. *Chem. Commun.* **2010**, *46*, 1994−2006.
(24) Murale, D. P.; Lee, K. M.; Kim, K.; Churchill, D. G. Facile "One Pot" Route to the Novel Benzazulene-Type Dye Class: Asymmetric, Derivatizable, 5-7-6 Fused Ring Puckered Half BODIPY Design. *Chem. Commun.* **2011**, *47*, 12512−12514.
(25) Yamamoto, K.; Harada, T.; Nakazaki, M.; Naka, T.; Kai, Y.; Harada, S.; Kasai, N. Synthesis and Characterization of [7]Circulene1. *J. Am. Chem. Soc.* **1983**, *105*, 7171−7172.
(26) Fukui, N.; Kim, T.; Kim, D.; Osuka, A. Porphyrin Arch-Tapes: Synthesis, Contorted Structures, and Full Conjugation. *J. Am. Chem. Soc.* **2017**, *139*, 9075−9088.
(27) Luo, J.; Xu, X.; Mao, R.; Miao, Q. Curved Polycyclic Aromatic Molecules That Are π-Isoelectronic to Hexabenzocoronene. *J. Am. Chem. Soc.* **2012**, *134*, 13796−13803.
(28) Hayakawa, S.; Kawasaki, A.; Hong, Y.; Uraguchi, D.; Ooi, T.; Kim, D.; Akutagawa, T.; Fukui, N.; Shinokubo, H. Inserting Nitrogen: An Effective Concept to Create Nonplanar and Stimuli-Responsive Perylene Bisimide Analogues. *J. Am. Chem. Soc.* **2019**, *141*, 19807−19816.
(29) Saito, S.; Nobusue, S.; Tsuzaka, E.; Yuan, C.; Mori, C.; Hara, M.; Seki, T.; Camacho, C.; Irle, S.; Yamaguchi, S. Light-Melt Adhesive Based on Dynamic Carbon Frameworks in a Columnar Liquid-Crystal Phase. *Nat. Commun.* **2016**, *7*, 12094.
(30) Żyła, M.; Gońka, E.; Chmielewski, P. J.; Cybińska, J.; Stępień, M. Synthesis of a Peripherally Conjugated 5-6-7 Nanographene. *Chem. Sci.* **2016**, *7*, 286−294.
(31) Hensel, T.; Trpcevski, D.; Lind, C.; Grosjean, R.; Hammershøj, P.; Nielsen, C. B.; Brock-Nannestad, T.; Nielsen, B. E.; Schau-Magnussen, M.; Minaev, B.; et al. Diazadioxa[8]Circulenes: Planar Antiaromatic Cyclooctatetraenes. *Chem.—Eur. J.* **2013**, *19*, 17097−17102.
(32) Rhodamine B https://omlc.org/spectra/PhotochemCAD/html/009.html (accessed Jan 16, 2020).
(33) Perekalin, V. V.; Savost'yanova, M. V.; Morozova, R. I. Study of the Absorption Spectra of Selected Di- and Triphenylmethane Derivatives (Russ.). *Zh. Obshch. Khim.* **1952**, *22*, 821−829.
(34) Mikheev, Y. A.; Guseva, L. N.; Ershov, Y. A. The Optical Properties of Triphenylmethane Dye Molecules and Chromogens. *Russ. J. Phys. Chem. A* **2008**, *82*, 1580−1588.
(35) Nagasawa, Y.; Ando, Y.; Okada, T. Solvent Dependence of Ultrafast Ground State Recovery of the Triphenylmethane Dyes, Brilliant Green and Malachite Green. *Chem. Phys. Lett.* **1999**, *312*, 161−168.
(36) Bagchi, B.; Fleming, G. R.; Oxtoby, D. W. Theory of Electronic Relaxation in Solution in the Absence of an Activation Barrier. *J. Chem. Phys.* **1983**, *78*, 7375−7385.
(37) Xie, B.-B.; Xia, S.-H.; Liu, L.-H.; Cui, G. Surface-Hopping Dynamics Simulations of Malachite Green: A Triphenylmethane Dye. *J. Phys. Chem. A* **2015**, *119*, 5607−5617.
(38) Nakayama, A.; Taketsugu, T. Ultrafast Nonradiative Decay of Electronically Excited States of Malachite Green: Ab Initio Calculations. *J. Phys. Chem. A* **2011**, *115*, 8808−8815.
(39) Wu, E. C.; Ge, Q.; Arsenault, E. A.; Lewis, N. H. C.; Gruenke, N. L.; Head-Gordon, M. J.; Fleming, G. R. Two-Dimensional Electronic-Vibrational Spectroscopic Study of Conical Intersection Dynamics: An Experimental and Electronic Structure Study. *Phys. Chem. Chem. Phys.* **2019**, *21*, 14153−14163.
(40) Jones, G.; Yan, D.; Hu, J.; Wan, J.; Xia, B.; Vullev, V. I. Photoinduced Electron Transfer in Arylacridinium Conjugates in a Solid Glass Matrix. *J. Phys. Chem. B* **2007**, *111*, 6921−6929.
(41) Hansch, C.; Leo, A.; Taft, R. W. A Survey of Hammett Substituent Constants and Resonance and Field Parameters. *Chem. Rev.* **1991**, *91*, 165−195.
(42) Delgado, J. C.; Selsby, R. G. Density Functional Theory Calculations on Rhodamine B and Pinacyanol Chloride. Optimized Ground State, Dipole Moment, Vertical Ionization Potential, Adiabatic Electron Affinity and Lowest Excited Triplet State. *Photochem. Photobiol.* **2013**, *89*, 51−60.
(43) Setiawan, D.; Kazaryan, A.; Martoprawiro, M. A.; Filatov, M. A First Principles Study of Fluorescence Quenching in Rhodamine B Dimers: How Can Quenching Occur in Dimeric Species? *Phys. Chem. Chem. Phys.* **2010**, *12*, 11238−11244.
(44) Wang, L.; Neumann, H.; Beller, M. Palladium-Catalyzed Methylation of Nitroarenes with Methanol. *Angew. Chem., Int. Ed.* **2019**, *58*, 5417−5421.

https://dx.doi.org/10.1021/acs.joc.0c00414
J. Org. Chem. 2020, 85, 5973−5980